

---

# GP-Tree: A Gaussian Process Classifier for Few-Shot Incremental Learning

---

Idan Achituve<sup>1</sup> Aviv Navon<sup>1</sup> Yochai Yemini<sup>1</sup> Gal Chechik<sup>1,2</sup> Ethan Fetaya<sup>1</sup>

## Abstract

Gaussian processes (GPs) are non-parametric, flexible, models that work well in many tasks. Combining GPs with deep learning methods via deep kernel learning is especially compelling due to the strong expressive power induced by the network. However, inference in GPs, whether with or without deep kernel learning, can be computationally challenging on large datasets. Here, we propose *GP-Tree*, a novel method for multi-class classification with Gaussian processes and deep kernel learning. We develop a tree-based hierarchical model in which each internal node of the tree fits a GP to the data using the Pólya-Gamma augmentation scheme. As a result, our method scales well with both the number of classes and data size. We demonstrate our method effectiveness against other Gaussian process training baselines, and we show how our *general* GP approach is easily applied to incremental few-shot learning and reaches state-of-the-art performance.

## 1. Introduction

Gaussian processes (GP) are a popular Bayesian non-parametric approach that enjoys a closed-form marginal likelihood, thus avoiding one of the major computational difficulties of many Bayesian approaches. However, several obstacles still persist, making it hard to successfully apply GPs to certain problems. First, GP performance heavily depends on the kernel function used. In domains such as images, where common kernels are not a good measure of semantic similarity, this can hinder performance. This problem is commonly addressed by deep kernel learning (Wilson et al., 2016a) where GPs are combined with the expressive power of modern neural networks and learn a useful kernel function from data.

Second, computing the marginal likelihood involves storing and inverting an  $n \times n$  kernel matrix where  $n$  is the number of training examples. This can limit exact inference on

large datasets, especially when combined with deep kernel learning where the kernel needs to be re-computed at each iteration. A common approach to handle large datasets is to learn a small set of inducing points, which act as a proxy for the training data (Snelson & Ghahramani, 2006).

While extensive work has been done on handling these challenges for Gaussian process regression, comparatively little has been done on how to scale Gaussian process *classification* (see Liu et al., 2020a, for a recent review). This is partly because the categorical distribution on the target variable results in non-Gaussian posteriors and we no longer have closed-form marginal likelihood. One appealing approach to address this obstacle is the Pólya-Gamma augmentation (Polson et al., 2013). In the Pólya-Gamma augmentation, the posterior becomes Gaussian when conditioned on the augmented Pólya-Gamma variable. However, this augmentation was designed for binary classification tasks. Since then, several extensions to multi-class classification have been proposed (Linderman et al., 2015; Galy-Fajou et al., 2020; Snell & Zemel, 2020). However, as we will show empirically their performance degrades as the number of target classes increases.

In this study, we present a novel method for Gaussian process classification (GPC) that is designed to handle both small and large datasets. Importantly, it is also designed to handle a large number of classes. We develop a tree-based model in which each node solves a binary classification task using a Gaussian process and the Pólya-Gamma augmentation scheme. We term our method *GP-Tree*. GP-Tree has great flexibility as it allows us to take samples from the exact posterior with Gibbs sampling, or apply variational inference and use the inducing point approximation. To train GP-Tree on large-scale image classification tasks we further combine it with deep kernel learning, and we show how on this setup as well, GP-Tree is superior to popular GPC methods.

Finally, we apply GP-Tree to the incremental few-shot learning challenges (Tao et al., 2020). In incremental few-shot learning, we assume that the data come sequentially. Initially, the learner is presented with many samples from some base classes. Then at each new iteration it has access only to a new, small, dataset that originated from novel classes not seen during previous iterations. Here the challenges are two-

---

<sup>1</sup>Bar-Ilan University, Israel <sup>2</sup>Nvidia, Israel. Correspondence to: Idan Achituve <idan.achituve@biu.ac.il>.

fold, generalizing from a small number of training points for the novel classes and avoiding catastrophic forgetting of the base classes. We claim that Gaussian processes are a good fit for this problem. The inducing points, which basically serve as a small proxy for the training data, can help mitigate the catastrophic forgetting problem, and GPs generalize well from small datasets due to their Bayesian nature. Indeed we show that once we get GPs to scale and successfully train on the base classes, our GP approach is competitive on incremental few-shot benchmarks and achieves state-of-the-art performance for large number of novel classes without *any* modifications or fine-tuning.

Thus, we make the following novel contributions: (1) We show how current Gaussian process classification methods struggle when the number of classes to be learned is large; (2) We present a novel method for Gaussian process classification that is designed to handle a large number of classes and datasets based on the Pólya-Gamma augmentation; (3) We present GPs as a promising new research direction for few-shot incremental learning; (4) We achieve state-of-the-art results when the number of classes is high on two benchmark datasets designed for few-shot incremental learning.

## 2. Background

### 2.1. Notation

We denote vectors with bold lower-case font, e.g.  $\mathbf{x}$ , and matrices with capital bold font, e.g.  $\mathbf{X}$ . Given a dataset  $(\mathbf{x}_1, y_1), \dots, (\mathbf{x}_n, y_n)$ , we denote by  $\mathbf{y} = [y_1, \dots, y_n]^T$  the vector of labels, and by  $\mathbf{X} \in \mathbb{R}^{n \times d}$  the design matrix whose  $i^{\text{th}}$  row is  $\mathbf{x}_i$ . In the classification case, each  $y_i$  takes a value from  $\{1, \dots, C\}$  class labels.

### 2.2. Gaussian Processes

In Gaussian process learning we assume the mapping from the input points to the target values is via a latent function  $f$ . The target values are assumed to be independent when conditioned on the latent function, i.e.,  $p(\mathbf{y}|\mathbf{X}, f) = \prod_{i=1}^n p(y_i|f(\mathbf{x}_i))$ . The latent function is assumed to follow a Gaussian process prior  $f \sim \mathcal{GP}(m(\mathbf{x}), k(\mathbf{x}, \mathbf{x}'))$ , where the evaluation vector of  $f$  on  $\mathbf{X}$ ,  $\mathbf{f} = [f(\mathbf{x}_1), \dots, f(\mathbf{x}_n)]^T$ , has a Gaussian distribution  $\mathbf{f} \sim \mathcal{N}(\boldsymbol{\mu}, \mathbf{K})$ , where  $\boldsymbol{\mu}_i = m(\mathbf{x}_i)$  and  $\mathbf{K}_{ij} = k(\mathbf{x}_i, \mathbf{x}_j)$ . The mean  $m$  is commonly taken to be the constant zero function, and the kernel  $k(\mathbf{x}, \mathbf{x}')$  is a positive semi-definite function.

Let  $\mathbf{X}, \mathbf{y}$  be the training data, and let  $f_*$  be the evaluation of  $f$  on a novel point  $\mathbf{x}_*$ . In the regression case, where we assume  $p(y|\mathbf{x}, f) = \mathcal{N}(f(\mathbf{x}), \sigma^2)$ , the predictive distributions,  $p(f_*|\mathbf{X}, \mathbf{y}, \mathbf{x}_*)$  and  $p(y_*|\mathbf{X}, \mathbf{y}, \mathbf{x}_*) = \int p(f_*|\mathbf{X}, \mathbf{y}, \mathbf{x}_*)p(y_*|f_*)df_*$ , are Gaussians whose param-

eters have a closed-form expression. Specifically,

$$\begin{aligned} p(f_*|\mathbf{X}, \mathbf{y}, \mathbf{x}_*) &= \mathcal{N}(\mu_*, \sigma_*), \\ \mu_* &= \mathbf{k}_*^T (\mathbf{K} + \sigma \mathbf{I})^{-1} \mathbf{y}, \\ \sigma_* &= k(\mathbf{x}_*, \mathbf{x}_*) - \mathbf{k}_*^T (\mathbf{K} + \sigma \mathbf{I})^{-1} \mathbf{k}_*, \end{aligned} \quad (1)$$

where  $\mathbf{k}_*[i] = k(\mathbf{x}_*, \mathbf{x}_i)$ ,  $\mathbf{K}[i, j] = k(\mathbf{x}_i, \mathbf{x}_j)$ . This closed-form solution allows us to avoid the costly marginalization step; however, it entails the inversion of an  $n \times n$  matrix which can be expensive to compute for large datasets.

In deep kernel learning (Wilson et al., 2016a), the kernel over the input data points is commonly in the form of a fixed kernel on an embedding learned by a deep neural network  $g_\theta$ , e.g.,  $k_\theta(\mathbf{x}, \mathbf{x}') = \exp(-\|g_\theta(\mathbf{x}) - g_\theta(\mathbf{x}')\|^2/\ell)$ . Therefore, the closed form inference is of even greater importance as it allows us to easily backpropagate through the GP inference.

### 2.3. Pólya-Gamma Augmentation

When applying GPs to classification tasks, the likelihood  $p(y|f(\mathbf{x}_i))$  is no longer Gaussian. The predictive distributions are also no longer Gaussian and we do not have a closed-form solution for them. To overcome this limitation, several methods were offered based on the Pólya-Gamma augmentation (Polson et al., 2013) to model the discrete likelihoods in GPs (Linderman et al., 2015; Wenzel et al., 2019; Galy-Fajou et al., 2020; Snell & Zemel, 2020). The Pólya-Gamma augmentation hinges on the following identity

$$\frac{(e^\psi)^a}{(1 + e^\psi)^b} = 2^{-b} e^{\kappa\psi} \mathbb{E}_\omega [e^{-\omega\psi^2/2}], \quad (2)$$

where  $\kappa = a - b/2$  and  $\omega$  has the Pólya-Gamma distribution  $\omega \sim PG(b, 0)$ .

Suppose we have a binary classification task with  $y \in \{0, 1\}$ , and we are given a vector of latent function values  $\mathbf{f}$ , the likelihood can be written as,

$$p(\mathbf{y}|\mathbf{f}) = \prod_{j=1}^n \sigma(f_j)^{y_j} (1 - \sigma(f_j))^{1-y_j} = \prod_{j=1}^n \frac{e^{y_j f_j}}{1 + e^{f_j}}. \quad (3)$$

We can now use Eq. 2 to introduce auxiliary Pólya-Gamma variables (one per sample) such that we recover Eq. 3 by marginalizing them out. If instead we sample the Pólya-Gamma variables  $\boldsymbol{\omega}$  we get the following posteriors:

$$\begin{aligned} p(\mathbf{f}|\mathbf{y}, \boldsymbol{\omega}) &= \mathcal{N}(\mathbf{f}|\boldsymbol{\Sigma}(\mathbf{K}^{-1}\mathbf{m} + \boldsymbol{\kappa}), \boldsymbol{\Sigma}), \\ p(\boldsymbol{\omega}|\mathbf{y}, \mathbf{f}) &= PG(\mathbf{1}, \mathbf{f}) \end{aligned} \quad (4)$$

where,  $\boldsymbol{\kappa}_j = y_j - 1/2$ ,  $\boldsymbol{\Sigma} = (\mathbf{K}^{-1} + \boldsymbol{\Omega})^{-1}$ , and  $\boldsymbol{\Omega} = \text{diag}(\omega_j)$ . We can now sample from  $p(\mathbf{f}, \boldsymbol{\omega}|\mathbf{X}, \mathbf{y})$  using block Gibbs sampling and get Monte-Carlo estimations of the marginal and predictive distributions.

## 2.4. Inducing Points

One major limitation of exact inference on GPs is that it compels us to store the entire training set, and invert an  $n \times n$  matrix  $\mathbf{K}_{nn}$ . A common solution to this problem is to use inducing points (Snelson & Ghahramani, 2006). Instead of applying the GP inference formulas on the real training data, we apply them on  $m \ll n$  pseudo-inputs  $\bar{\mathbf{X}}$ , whose locations are trainable parameters. This can be done while inverting only an  $m \times m$  matrix which allows us to control the computational cost.

Our approach closely follows the inducing points method for classification with Pólya-Gamma augmentation presented in (Wenzel et al., 2019) for binary classification. Here we define  $\bar{\mathbf{X}}$  as the inducing locations/inputs and  $\bar{\mathbf{f}}$  as the latent function value evaluated on  $\bar{\mathbf{X}}$ . We have,

$$p(\bar{\mathbf{f}}) = \mathcal{N}(0, \mathbf{K}_{mm}), \quad (5)$$

$$\begin{aligned} p(\mathbf{f}|\bar{\mathbf{f}}) &= \mathcal{N}(\mathbf{K}_{nm}\mathbf{K}_{mm}^{-1}\bar{\mathbf{f}}, \mathbf{Q}_{nn}), \\ \mathbf{Q}_{nn} &= \mathbf{K}_{nn} - \mathbf{K}_{nm}\mathbf{K}_{mm}^{-1}\mathbf{K}_{mn} \end{aligned} \quad (6)$$

$$p(\mathbf{y}, \boldsymbol{\omega}, \mathbf{f}, \bar{\mathbf{f}}) = p(\mathbf{y}|\mathbf{f}, \boldsymbol{\omega})p(\mathbf{f}|\bar{\mathbf{f}})p(\bar{\mathbf{f}})p(\boldsymbol{\omega}) \quad (7)$$

where  $\mathbf{K}_{mm}$  is the kernel matrix on the inducing locations and  $\mathbf{K}_{nm}$  is the cross-kernel matrix between inducing locations and the inputs. While  $p(\bar{\mathbf{f}}|\mathbf{y}, \boldsymbol{\omega})$  is Gaussian using the Pólya-Gamma augmentation. The distribution after marginalization,  $p(\bar{\mathbf{f}}|\mathbf{y})$ , is not in general Gaussian. Following (Hensman et al., 2015), in (Wenzel et al., 2019) a variational inference approach was proposed with a variational distribution  $q(\boldsymbol{\omega}, \mathbf{f}) = q(\boldsymbol{\omega})q(\bar{\mathbf{f}})$  with Pólya-Gamma  $q(\boldsymbol{\omega})$  and Gaussian  $q(\bar{\mathbf{f}})$ . They then optimize the variational parameters and  $\bar{\mathbf{X}}$  using natural gradient descent.

## 3. Method

Now we will describe our method to train GP classifiers that use deep kernel learning, and scale to large training sets and a large number of classes. Next, we will show how we can apply it to novel classes without training any new parameters.

### 3.1. Hierarchical Classification

In (Linderman et al., 2015) the authors utilize the Pólya-Gamma augmentation, which was designed for binary labels, for multinomial and multi-class classification problems by using the stick-breaking process. They turn the multi-class classification task into a sequence of  $C - 1$  binary classification tasks where  $y^j = 1$  if the original label is  $j$  and  $y^j = 0$  if the original label is larger than  $j$ . We can then apply  $C - 1$  independent latent Gaussian processes, one for each binary classification task. The vector of latent processes values at

the  $i^{th}$  example is denoted by  $\mathbf{f}_i = (f_i^1, \dots, f_i^{C-1})$ , and we have the following likelihood:

$$p(y_i = c|\mathbf{f}_i) = \sigma(f^c) \prod_{k < c} (1 - \sigma(f^k)) \quad (8)$$

where the remaining probability mass is assigned to the  $C^{th}$  class. While the stick-breaking formulation allows us to break the multiclass classification problem into a sequence of binary classification tasks, as we will show in section 5.1, its performance degrades with the number of classes.

As can be seen in Figure 1(a), one can think of the stick-breaking process as a hierarchical classification with an extremely unbalanced tree. This sequential structure can be severely suboptimal for two reasons: (1) The number of binary classification tasks needed to classify a data point grows linearly with the number of classes instead of logarithmically for a perfectly balanced tree; (2) Not all label splits result in equally hard binary classification tasks, and the stick-breaking process simply uses the default label ordering.

We, therefore, propose to use a tree-structured hierarchical classification instead of the sequential alternative, in which we try to find a tree structure that results in easy to learn binary tasks. Conceptually, we create a tree by splitting the data recursively by classes until we get to single class leaves. More formally, at the root we partition the classes  $\{1, \dots, C\}$  into two sets  $C_l$  and  $C_r$  such that  $C_l \cap C_r = \emptyset$  and,  $C_l \cup C_r = \{1, \dots, C\}$ . We then define  $D_l$  and  $D_r$  as the data points associated with the  $C_l$  classes and  $C_r$  classes respectively. We then assign  $D_l$  to the left child of the root node and  $D_r$  to the right one. We recursively apply the same operation at each node until we are left with single class leaf nodes. Thus, a binary tree is formed (not necessarily a perfectly balanced one), see Figure 1(b) for an example. We then fit a binary GP classification model to each internal node of the tree that makes a binary decision where all the  $C_l$  classes are grouped into one class and all the  $C_r$  classes are grouped into another class. We name our model *GP-Tree*.

The model quality depends on how we partition the data, namely the tree building processes described above. A naive approach would be to use a random balanced binary tree however, this strategy is sub-optimal. We propose the following procedure: We first compute a representative prototype of each class by taking the mean of representation of all samples belonging to that class. We then normalize the vectors to have unit length and apply divisive hierarchical clustering. We recursively split each node, by using  $k$ -means++ clustering (Arthur & Vassilvitskii, 2007) with  $k = 2$  on the class prototype vectors, until we are left with single class leaves.

We fit a GP at each internal node which makes a binary deci-

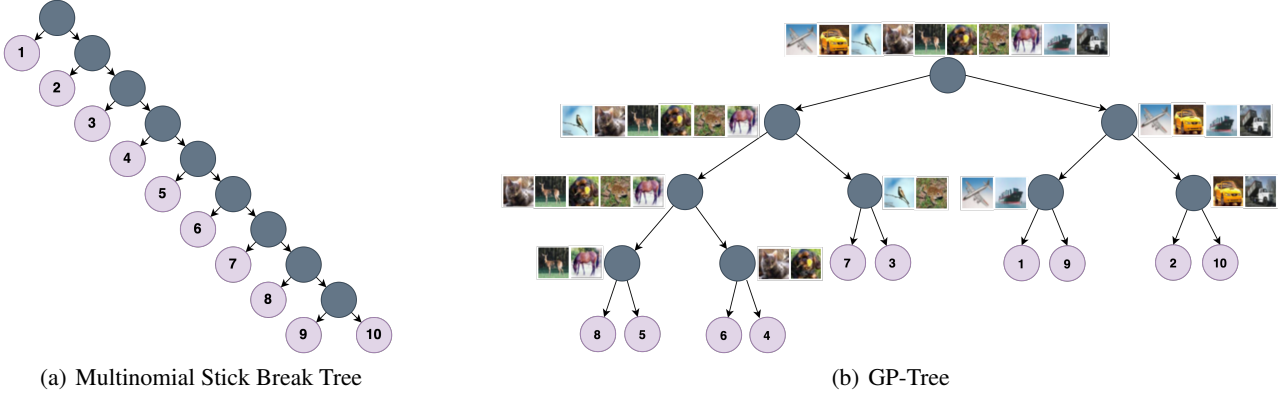


Figure 1. The trees corresponding to the multinomial stick break model (left) and to the GP-Tree model (right) for CIFAR-10. The multinomial stick break generates an unbalanced tree in which the order of the classes is arbitrary. GP-Tree, on the other hand, generates a more balanced tree that is divided by the semantic meaning of the classes. For example, motorized vehicles are on the right subtree of the root node while animals are on the left one. This semantic partition is pronounced at all of the tree levels.

sion based on the data associated with that node. We denote the GP associated with node  $v_i$  by  $f_{v_i} \sim \mathcal{GP}(\mathbf{m}_{v_i}, \mathbf{K}_{v_i})$ , and all of the GPs in the tree with  $\mathcal{F}$ . The likelihood of a data point having the class  $c$  is given by the unique path  $P^c$  from the root to the leaf node corresponding to that class:

$$p(y = c | \mathcal{F}) = \prod_{v_i \in P^c} \sigma(f_{v_i})^{y_{v_i}} (1 - \sigma(f_{v_i}))^{1 - y_{v_i}} \quad (9)$$

where  $y_{v_i} = 1$  if the path goes left at  $v_i$  and zero otherwise.

### 3.2. Inference at the Node Level

Since the likelihood in Eq. 9 factorizes over the nodes, we may look at the individual components separately. In the following we omit subscript  $v_i$  for clarity however, all datum and quantities are those that belong to a specific node  $v_i$ . In general, we can perform inference on each tree node with either Gibbs sampling or variational inference (VI). For training on large datasets with deep kernel learning and inducing points, we found the variational approach to scale better, as the inducing points posterior depends on the entire dataset. However, for incremental few-shot learning, the Gibbs sampling method is very suitable for novel classes as no new parameters are required.

For Gibbs sampling, we use the posterior probabilities introduced in section 2.3. At each node, we can use block-Gibbs sampling to sample  $\omega$  and  $\mathbf{f}$  and do inference either with the marginal or predictive distributions described next.

The augmented marginal likelihood is given by

$$p(\mathbf{y} | \omega, \mathbf{X}) = \int p(\mathbf{y} | \omega, \mathbf{X}, \mathbf{f}) p(\mathbf{f}) d\mathbf{f} \quad (10)$$

$$\propto \mathcal{N}(\Omega^{-1} \boldsymbol{\kappa} | \mathbf{m}, \mathbf{K} + \Omega^{-1})$$

The augmented predictive distribution on new datum  $\mathbf{x}_*$ :

$$p(y_* | \mathbf{x}_*, \mathbf{X}, \mathbf{y}, \omega) = \int p(y_* | f_*) p(f_* | \mathbf{x}_*, \mathbf{X}, \mathbf{y}, \omega) df_* \quad (11)$$

$$p(f_* | \mathbf{x}_*, \mathbf{X}, \mathbf{y}, \omega) = \mathcal{N}(f_* | \mu_*, \Sigma_*)$$

$$\mu_* = \mathbf{k}_* (\Omega^{-1} + \mathbf{K})^{-1} \Omega^{-1} \boldsymbol{\kappa} \quad (12)$$

$$\Sigma_* = \mathbf{k}_{**} - \mathbf{k}_* (\Omega^{-1} + \mathbf{K})^{-1} \mathbf{k}_*^T$$

The integral in Eq. 11 is intractable but can be computed numerically with 1D Gaussian-Hermite quadrature.

Alternatively to the Gibbs sampling, we may apply variational inference at each node. We define  $\bar{\mathbf{X}}$  as the learned pseudo-inputs and  $\bar{\mathbf{y}}$  as their associated class labels.  $\bar{\mathbf{X}}$  are defined at the tree level and are shared by all relevant nodes. For each node we define the variational distributions  $q(\omega) = PG(\mathbf{1}, \mathbf{c})$  and  $q(\bar{\mathbf{f}}) = \mathcal{N}(\bar{\mathbf{f}} | \boldsymbol{\mu}, \tilde{\boldsymbol{\Sigma}})$ , where  $\mathbf{c}, \boldsymbol{\mu}, \tilde{\boldsymbol{\Sigma}}$  are learnable parameters. The variational lower bound to the marginal likelihood is:

$$\mathcal{L}(\mathbf{c}, \boldsymbol{\mu}, \boldsymbol{\Sigma}) = \mathbb{E}_{p(\bar{\mathbf{f}} | \bar{\mathbf{f}}) q(\bar{\mathbf{f}}) q(\omega)} [\log p(\mathbf{y} | \omega, \mathbf{f})] - \text{KL}(q(\bar{\mathbf{f}} | \omega) || p(\bar{\mathbf{f}} | \omega)) \quad (13)$$

which has a closed-form expression. We can then learn the model parameters and the variational parameters by maximizing the variational lower bound in Eq. 13. The explicit form of the Eq. 13 and the update rules for the variational parameters were adapted from (Wenzel et al., 2019) and are presented in supplementary section A.

To make predictions using the variational distribution we can replace the exact predictive posterior  $p(f_* | \mathbf{x}_*, \mathbf{X}, \mathbf{y})$ , with

the approximation:

$$\begin{aligned}
 p(f_* | \mathbf{x}_*, \bar{\mathbf{X}}, \bar{\mathbf{y}}) &\approx \int p(f_* | \bar{\mathbf{f}}, \mathbf{x}_*) q(\bar{\mathbf{f}}) d\bar{\mathbf{f}} \\
 &= \mathcal{N}(f_* | \mu_*, \Sigma_*) \\
 \mu_* &= \mathbf{k}_{*m} \mathbf{K}_{mm}^{-1} \boldsymbol{\mu} \\
 \Sigma_* &= k_{**} - \mathbf{k}_{*m} (\boldsymbol{\Sigma} \mathbf{K}_{mm}^{-1} - \mathbf{I}) \mathbf{k}_{*m}^T
 \end{aligned} \tag{14}$$

Where,  $\mathbf{k}_{*m}$  denotes the kernel vector between the test point and the inducing points, and  $k_{**}$  denotes the kernel value at the test point. Similarly to the sampling case, we can get  $p(y_* | \mathbf{x}_*, \bar{\mathbf{X}}, \bar{\mathbf{y}})$  by taking an integral over  $f_*$  and compute it numerically with 1D Gaussian-Hermite quadrature.

### 3.3. Full Learning of the Tree

We discussed how to learn and perform inference on a single node, we will now describe how to train the full tree model. For the full tree we need to learn the joint pseudo-inputs and the per-node variational distributions when using variational inference. Optimizing the full tree splits into the separate marginal likelihood of all examples and all the nodes on the path from the root to the leaf nodes:

$$\begin{aligned}
 \mathcal{L} &= \sum_{j=1}^n \log p(y_j | \mathbf{x}_j, \bar{\mathbf{X}}, \bar{\mathbf{y}}) \\
 &= \sum_{j=1}^n \sum_{v_i \in P^{y_j}} \log p(y_{v_i} | \mathbf{x}_j, \bar{\mathbf{X}}, \bar{\mathbf{y}})
 \end{aligned} \tag{15}$$

Since we cannot directly optimize this loss, we optimize the lower bound of it given in Eq. 13.

Our method can be easily integrated with deep kernel learning. We simply superimpose the tree-based GP on an embedding layer of a neural network and learn the network parameters  $\theta$  as well. In the case we have inducing points we may define the inducing inputs in the input space or at the feature space. We found that setting them in the feature space yielded better performance, and also requires less memory. We initialized their location at the beginning of training using k-means++ on the embedding of the data samples. We empirically found that it is beneficial to start the training process with a few epochs of standard training using cross-entropy loss before building the GP tree and transitioning to learning with it. Finally, to apply predictions in the original multi-class problem, the prediction for a data point  $x_*$  is given as the product of predictive distributions from the root node to leaf node corresponding to each class. We summarize the learning algorithm of GP-Tree in supplementary section B.

### 3.4. GP-Tree for Few-Shot Class Incremental Learning

In class-incremental learning, we are given a sequence of labeled datasets  $D_1, D_2, \dots, D_T$  each sampled from a disjoint

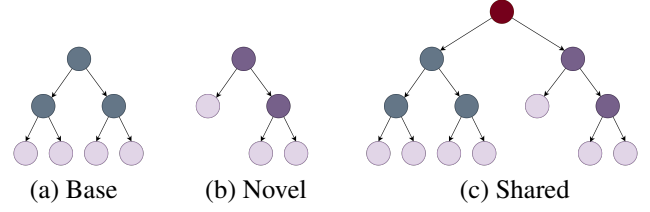


Figure 2. Tree expansion for novel classes: (a) A tree that was learned on the base classes; (b) On a novel session, we first build a tree from novel classes representations; (c) Next we connect the trees using a shared root node.

set of classes  $C_1, \dots, C_T$ . At each timestamp  $t$  the model has access to dataset  $D_t$  and the previous model, and it is tasked with classifying all the previously seen classes  $\cup_{i=1}^t C_i$ . In the few-shot incremental learning (Ren et al., 2019; Tao et al., 2020), the base classes  $D_1$  have a large number of samples, but all of the following datasets ( $D_2$  onwards) have a limited amount of labeled data, e.g., 5 samples per class. Thus, after the model learned on the base classes it is tasked with learning new classes from few examples and without impairing the classification of previously seen classes whose data isn't available at that time, also known as catastrophic forgetting (McCloskey & Cohen, 1989). Gaussian processes are naturally well-suited for this challenge. Bayesian models are well known to generalize well from few examples (Snell & Zemel, 2020) and the inducing points can be used as a compact representation of the base classes that allows us to avoid catastrophic forgetting. As the Gaussian process is non-parametric we can classify new classes without fitting any new variables or tuning our previous network, which also mitigate the catastrophic forgetting problem.

At the initial phase of learning the base classes, we employ GP-Tree (with deep kernel learning) to learn this dataset by using VI, as described in section 3.3. We can view the inducing inputs, which are learned per-class, as 'exemplars' of the base classes, which are commonly learned or selected from the training set in incremental learning studies (He et al., 2018; Douillard et al., 2020).

When given data from novel classes, we freeze the neural network backbone and use the embedding representation of the new samples as new examples to the GP-Tree. Therefore, we just need to restructure the tree in order to account for the new classes. We retain the original tree that was learned on the base classes intact, and at each novel session, we build a sub-tree from the samples in sessions  $D_2, \dots, D_t$ . We then connect this sub-tree to the base classes tree with a shared root node and define a GP to it as well. See illustration in Figure 2. We use Gibbs sampling on all new nodes to avoid any parameter tuning after the initial training on the base classes. It is important to note that while we do save the inducing inputs and the novel samples representations

for future sessions, this is in line with other incremental learning works, e.g. (Douillard et al., 2020), that save a few samples per class. As we only save the embedding and not the original image we get lower memory costs, which in practice are negligible compared to storing the trained network weights.

We also note that this is a natural way to extend our classification to new classes and it was not tailored for the class-incremental few-shot scenario. Despite that, we show strong results compared to models designed specifically for this task, especially on later learning sessions.

#### 4. Related work

**Incremental learning.** Incremental learning (IL) aims at learning new data without forgetting old data, what is known as ‘catastrophic forgetting’ (McCloskey & Cohen, 1989). Recently, a large body of research was done in this direction however, to the best of our knowledge, there are no relevant studies on Incremental learning for classification tasks with GPs. Methods in this field can be categorized according to three types: (i) *Regularization based* approaches impose regularization methods on the network to maintain past knowledge (Goodfellow et al., 2014; Kirkpatrick et al., 2017; Lee et al., 2017; Chaudhry et al., 2018; Schwarz et al., 2018; Ren et al., 2019). For example, (Kirkpatrick et al., 2017) limit the update of the parameters when encountering new data based on the fisher matrix ; (ii) *Architectural based* methods suggest network architectures that are resilient to the catastrophic forgetting issue and are able to accommodate new tasks (Mallya et al., 2018; Mallya & Lazebnik, 2018; Yoon et al., 2018; Serra et al., 2018; Taitelbaum et al., 2019; jun Liu et al., 2020). For example, (Rusu et al., 2016) and following it (Yoon et al., 2018) expend the network with each new task. When applying parameters update the former freezes the previous network while the latter retrain part of it; (iii) *Rehearsal based* aims at preventing catastrophic forgetting by storing and replaying information from previous episodes (Rebuffi et al., 2017; Castro et al., 2018; Wu et al., 2018; Hou et al., 2019; Zhai et al., 2019; Liu et al., 2020b; jun Liu et al., 2020). (Rebuffi et al., 2017) introduced the class-incremental learning setup. They used exemplars to maintain information of past data and applied the nearest-mean-of-exemplars classification rule. In this paper, we follow the protocol suggested by (Tao et al., 2020) for few-shot class-incremental learning.

**Gaussian process classification.** In GPs for classification tasks the likelihood is no longer Gaussian and therefore approximation based approaches or Monte-Carlo based approaches are needed. Some classic non-augmentation based methods include the Laplace approximation (Williams & Barber, 1998), expectation-propagation (Minka, 2001), and the least square approach (Rifkin & Klautau, 2004). We

refer the readers to (Rasmussen & Williams, 2005) for a thorough review. Recently some approaches emerged that are based on the Pólya-Gamma augmentation (Polson et al., 2013). (Linderman et al., 2015) proposed to use the Pólya-Gamma in a stick-breaking process to reparameterize a multinomial distribution as a product of binomial distributions. (Wenzel et al., 2019) proposed to use Pólya-Gamma augmentation with variational inference for binary classification task. (Galy-Fajou et al., 2020) proposed to use the logistic softmax likelihood, and derived a conditionally conjugate model based on three augmentation steps which may degrade the performance due to the cascade of approximations. (Snell & Zemel, 2020) proposed to use the one-vs-each likelihood in a few shot setting. Their method does not scale well with the data and classes due to the inversion of a  $CN \times CN$  matrix.

**Scalable GPs.** In recent years some attempts were made to make GP classification more scalable. To handle large datasets (Snelson & Ghahramani, 2006) introduced the inducing points method. (Hoffman et al., 2013) developed a stochastic optimization process for VI. (Hensman et al., 2015) introduce a method for GPC within a variational inducing point framework. (Izmailov et al., 2018) uses Tensor Train decomposition for variational parameters that allows increasing dramatically the number of inducing points been used. Some methods applied GPC within the framework of deep kernel learning (Wilson et al., 2016a). (Wilson et al., 2016b) proposed to learn multiple GPs on an embedding space and combine them linearly before a Softmax function. Extending this method to the incremental learning setting is not immediate as there are learnable parameters for combining the classes. (Bradshaw et al., 2017) used a GP with the Robust-Max likelihood to achieve robustness against adversarial examples. This method doesn’t scale well with the number of classes as we will show in section 5.2. Also, unlike our method, both methods do not allow Gibbs sampling for cases in which the datasets are small.

**Hierarchical stick break** (Adams et al., 2010) proposed a tree-based stick break for clustering as an alternative to the standard sequential stick break. (Nassar et al., 2019) proposed to use a tree-structure stick break for linear dynamical systems. Both methods did not include any GP components and do not have the flexibility of our model to apply inference with VI.

#### 5. Experiments

In our experiments, we first examine several aspects of our method compared to previous common GPC methods (sections 5.1 & 5.2). Then we evaluate GP-Tree on the setting of class incremental few-shot learning (section 5.3). In the supplementary material we provide full implementation details (section C), ablation study, and further analysis (section D).

Table 1. Test accuracy on CUB-200-2011. Average over 10 runs ( $\pm$  SEM). In bold - best results when statistically significant ( $p=0.05$ ).

Method	Number of Classes								
	4	6	8	10	20	30	40	50	60
SBM-GP	96.98 $\pm$ 0.5	95.55 $\pm$ 0.9	92.11 $\pm$ 0.8	91.04 $\pm$ 0.7	83.59 $\pm$ 0.5	77.63 $\pm$ 0.9	67.03 $\pm$ 0.8	64.20 $\pm$ 1.0	60.69 $\pm$ 1.0
OVE	97.33 $\pm$ 0.5	96.60 $\pm$ 0.9	94.70 $\pm$ 0.8	93.05 $\pm$ 0.8	–	–	–	–	–
LSM	97.30 $\pm$ 0.9	96.95 $\pm$ 0.8	95.16 $\pm$ 0.8	93.09 $\pm$ 0.9	89.23 $\pm$ 1.3	84.44 $\pm$ 0.6	72.90 $\pm$ 1.2	69.82 $\pm$ 0.9	65.53 $\pm$ 0.9
GP-Tree Rnd. (ours)	97.80 $\pm$ 0.8	95.96 $\pm$ 0.7	93.49 $\pm$ 0.9	92.07 $\pm$ 1.1	85.32 $\pm$ 1.6	77.45 $\pm$ 1.0	68.97 $\pm$ 0.8	62.77 $\pm$ 1.2	58.49 $\pm$ 0.8
GP-Tree (ours)	97.93 $\pm$ 0.7	97.15 $\pm$ 0.6	94.67 $\pm$ 0.9	93.57 $\pm$ 0.9	88.77 $\pm$ 1.4	83.87 $\pm$ 0.8	<b>75.66<math>\pm</math>0.8</b>	<b>72.87<math>\pm</math>0.8</b>	<b>69.92<math>\pm</math>0.6</b>

### 5.1. Inference with Gibbs Sampling

As described in section 3, one option to do inference with GP-Tree is with Gibbs sampling. This method is preferable for novel sessions in incremental learning as we do not need to optimize the variational approximation and the data size is small. We evaluated GP-Tree in this setup on the fine-grained classification dataset, Caltech-UCSD Birds (CUB) 200-2011 (Welinder et al., 2010). The CUB dataset contains 200 classes of bird species in 11,788 images with approximately 30 examples per class in the training set. Here, we did not apply deep kernel learning, but rather we used the pre-trained features published by (Xian et al., 2018). This allowed us to only compare the inference part of our model.

We compared GP-Tree against the following baselines that introduced the Pólya-Gamma augmentation to get a conditionally conjugate likelihood: **(1) Stick Break Multinomial GP (SBM-GP)** (Linderman et al., 2015): which used the stick-breaking process to convert a multinomial likelihood to a product of binomial likelihoods **(2) Logistic-Softmax (LSM)** (Galy-Fajou et al., 2020) a recent method for GPC based on the logistic-softmax likelihood; and **(3) One-vs-Each (OVE)** (Snell & Zemel, 2020) a method for GPC proposed recently for the setup of few-shot learning. Because this method requires the inversion of a  $CN \times CN$  matrix, we were able to run it with only a few classes.

Table 1 compares GP-Tree against the baseline methods at increasing number of classes starting from 4 to 60 (out of 200). The results are the average test-set classification accuracy along with the standard error of the mean (SEM) over ten seeds which included randomization in the class selection. When the number of classes is small ( $\leq 30$ ) GP-Tree, LSM, and OVE are comparable. However, as the number of classes increases GP-Tree performs better. Table 1 also shows the results of a variant of the GP-Tree model in which a balanced tree is built based on randomly splitting the classes (**GP-Tree Rnd**). This variant performs similarly to the SBM-GP baseline, indicating the importance of the class split algorithm in GP-Tree. This is pronounced in Figure 1(b) that shows the tree generated by GP-Tree for CIFAR-10. The node partition is based on semantic similarity, e.g. the first split separates animals from vehicles.

### 5.2. Learning GPs with Deep Kernel Learning

Table 2. Test accuracy of GPs with Deep Kernel Learning

Method	CIFAR10	CIFAR100
GPDNN	81.16 $\pm$ 0.1	–
SV-DKL	92.51 $\pm$ 0.1	70.61 $\pm$ 0.2
GP-Tree (ours)	<b>92.71 <math>\pm</math> .05</b>	<b>72.07 <math>\pm</math> 0.1</b>

For evaluating GP-Tree with deep kernel learning we used the CIFAR-10 and CIFAR-100 datasets. Here we used only the VI variant of GP-Tree. We compared GP-Tree with the following popular baselines that also combined GPC with deep kernel learning: **(1) Stochastic Variational Deep Kernel Learning (SV-DKL)** (Wilson et al., 2016b) - which learned multiple GPs, each on a different subset of the embedding space, and combined them with the Softmax function; and **(2) GPDNN** (Bradshaw et al., 2017) which used the Robust-Max likelihood (Hernández-Lobato et al., 2011). We used ResNet-18 (He et al., 2016) as the backbone NN with an embedding layer of size 1024 and trained for 200 epochs. Table 2 shows the average accuracy across 3 seeds for both datasets along with the SEM. The comparison shows that both GP-Tree and SV-DKL achieve high accuracies with an advantage to GP-Tree on both datasets. We found that GPDNN was extremely sensitive to learning rate choice and the hyper-parameter controlling the probability of labeling error, and we could not get reasonable results for it on the CIFAR-100 dataset.

We note that the SV-DKL method is less suited for incremental learning, as the model includes a linear mapping followed by a softmax to produce the class distribution. That means that the associated parameters of new classes will need to be learned and risks catastrophic forgetting, unlike our approach where no new parameters are tuned.

### 5.3. Class-Incremental Few-Shot Learning

In this section, we evaluate GP-Tree on the challenging task of few-shot class-incremental learning (FSCIL). We compare with methods that were designed for this learning setup and show comparable, if not superior, results by simply applying GP-tree. This indicates that Gaussian processes

Table 3. Class-incremental few-shot learning results on CUB-200-2011. Test accuracy averaged over 10 runs.

Method	Sessions										
	1	2	3	4	5	6	7	8	9	10	11
iCaRL	68.68	52.65	48.61	44.16	36.62	29.52	27.83	26.26	24.01	23.89	21.16
EEIL	68.68	53.63	47.91	44.20	36.30	27.46	25.93	24.70	23.95	24.13	22.11
NCM	68.68	57.12	44.21	28.78	26.71	25.66	24.62	21.52	20.12	20.06	19.87
TOPIC	68.68	62.49	54.81	49.99	45.25	41.40	38.35	35.36	32.22	28.31	26.28
SDC	67.94	52.46	46.43	42.04	42.19	39.76	39.65	38.53	37.08	39.16	38.96
PODNet	<b>75.93</b>	<b>70.29</b>	<b>64.50</b>	49.00	45.90	43.00	41.33	40.56	40.09	40.59	39.30
GP-Tree (ours)	69.74	64.43	60.55	<b>56.01</b>	<b>52.73</b>	<b>49.95</b>	<b>47.68</b>	<b>46.09</b>	<b>43.82</b>	<b>42.5</b>	<b>41.09</b>

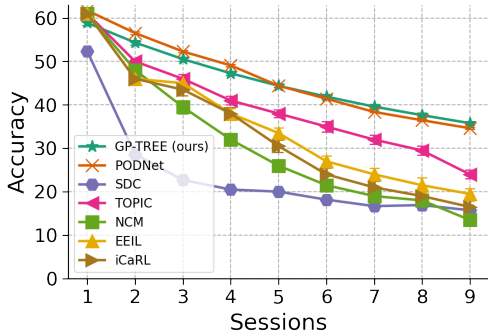


Figure 3. Class-incremental few-shot learning results on mini-ImageNet. Test set accuracy averaged over 10 runs.

in general and GP-Tree, in particular, are well suited and a natural approach to incremental few-shot learning.

We follow the benchmarks proposed in (Tao et al., 2020), using the CUB 200-2011 dataset, and mini-Imagenet (Deng et al., 2009), a 100-class subset of the Imagenet data used in few-shot studies (Finn et al., 2017). We adopt the 10-way 5-shot setting for CUB, choosing 100 base classes, and splitting the remaining 100 classes into ten incremental sessions. For mini-ImageNet, we follow the 5-way 5-shot, with 60 base classes, for a total of nine sessions.

Since the data splits made public by (Tao et al., 2020) did not include a validation set, we pre-allocate a small portion of the base classes dataset for the hyper-parameter tuning of all compared methods for both datasets. We provide additional experimental details in supplementary section C.3.

We compare GP-Tree with recent and leading FSCIL methods, the results of the following methods were taken from (Tao et al., 2020): (1) **iCaRL** (Rebuffi et al., 2017) that used exemplars of past data and applied the nearest-mean-of-exemplars classification; (2) **EEIL** (Castro et al., 2018) that used a distillation loss for old classes combined with a classification loss on all classes; (3) **NCM** (Hou et al., 2019) which combined a classification loss, a distillation loss over normalized embedding layer, and a margin ranking loss; (4) **TOPIC** (Tao et al., 2020) optimized a neural gas network

with classification loss, an anchor loss for less forgetting stabilization and a min-max loss to reduce overfitting. We also compare with two additional methods: (5) **SDC** (Yu et al., 2020) combined several losses to learn embedding representation and introduced a drift compensation to update previously computed prototypes. (6) **PODNet** (Douillard et al., 2020) uses a spatial-based distillation-loss and a representation consists of multiple proxy vectors per class.

The results for CUB are presented in Table 3 and for mini-ImageNet in Figure 3. On both datasets, we used the PyTorch implementation of ResNet-18 to be consistent with the results seen in (Tao et al., 2020). Results on mini-ImageNet could be improved with adapting NN architectures for smaller images, but we kept the standard ResNet-18 for comparability with (Tao et al., 2020). We also note that unlike on CUB, we were not able to get SDC to run well on mini-ImageNet, despite our best efforts.

The comparison shows that while PODNet outperforms all other methods during the first sessions, our GP-Tree achieves the best accuracy for the remaining of the sessions (4-11 in CUB and 5-9 in mini-ImageNet), where the challenges of avoiding catastrophic forgetting and few-shot learning becomes more difficult. These results give a good indication that using GPs can indeed handle these problems better than competing methods, but there is still room for improvement in how it handles the base classes.

## 6. Conclusion

In this work, we showed how common Gaussian process classification methods struggle when facing classification tasks with a large number of classes. We then presented our method, GP-tree, that can scale to a large number of classes and large datasets. GP-tree can be successfully combined with deep kernel learning. Finally, we showed how GP-tree can be directly applied to class-incremental few-shot learning challenges and achieves strong results. This indicates that Gaussian processes are a new and promising approach for this task.

## References

- Adams, R. P., Ghahramani, Z., and Jordan, M. I. Tree-structured stick breaking for hierarchical data. In *24th Annual Conference on Neural Information Processing Systems 2010, NIPS 2010*, 2010.
- Arthur, D. and Vassilvitskii, S. k-means++ the advantages of careful seeding. In *Proceedings of the eighteenth annual ACM-SIAM symposium on Discrete algorithms*, pp. 1027–1035, 2007.
- Bradshaw, J., Matthews, A. G. d. G., and Ghahramani, Z. Adversarial examples, uncertainty, and transfer testing robustness in Gaussian process hybrid deep networks. *arXiv preprint arXiv:1707.02476*, 2017.
- Castro, F. M., Marín-Jiménez, M. J., Guil, N., Schmid, C., and Alahari, K. End-to-end incremental learning. In *Proceedings of the European conference on computer vision*, pp. 233–248, 2018.
- Chaudhry, A., Dokania, P. K., Ajanthan, T., and Torr, P. H. Riemannian walk for incremental learning: Understanding forgetting and intransigence. In *Proceedings of the European Conference on Computer Vision*, pp. 532–547, 2018.
- Deng, J., Dong, W., Socher, R., Li, L.-J., Li, K., and Fei-Fei, L. Imagenet: A large-scale hierarchical image database. In *2009 IEEE conference on computer vision and pattern recognition*, pp. 248–255. Ieee, 2009.
- Douillard, A., Cord, M., Ollion, C., Robert, T., and Valle, E. PODNet: Pooled outputs distillation for small-tasks incremental learning. In *ECCV*, 2020.
- Finn, C., Abbeel, P., and Levine, S. Model-agnostic meta-learning for fast adaptation of deep networks. In *International Conference on Machine Learning*, pp. 1126–1135. PMLR, 2017.
- Galy-Fajou, T., Wenzel, F., Donner, C., and Opper, M. Multi-class Gaussian process classification made conjugate: Efficient inference via data augmentation. In *Uncertainty in Artificial Intelligence*, pp. 755–765. PMLR, 2020.
- Goodfellow, I. J., Mirza, M., Da, X., Courville, A. C., and Bengio, Y. An empirical investigation of catastrophic forgetting in gradient-based neural networks. *CoRR*, abs/1312.6211, 2014.
- He, C., Wang, R., Shan, S., and Chen, X. Exemplar-supported generative reproduction for class incremental learning. In *BMVC*, pp. 98, 2018.
- He, K., Zhang, X., Ren, S., and Sun, J. Deep residual learning for image recognition. In *Proceedings of the IEEE conference on computer vision and pattern recognition*, pp. 770–778, 2016.
- Hensman, J., Matthews, A., and Ghahramani, Z. Scalable variational Gaussian process classification. In *Artificial Intelligence and Statistics*, pp. 351–360. PMLR, 2015.
- Hernández-Lobato, D., Hernández-lobato, J., and Dupont, P. Robust multi-class Gaussian process classification. *Advances in neural information processing systems*, 24: 280–288, 2011.
- Hoffman, M. D., Blei, D. M., Wang, C., and Paisley, J. Stochastic variational inference. *Journal of Machine Learning Research*, 14(5), 2013.
- Hou, S., Pan, X., Loy, C. C., Wang, Z., and Lin, D. Learning a unified classifier incrementally via rebalancing. In *Proceedings of the IEEE/CVF Conference on Computer Vision and Pattern Recognition*, pp. 831–839, 2019.
- Izmailov, P., Novikov, A., and Kropotov, D. Scalable Gaussian processes with billions of inducing inputs via tensor train decomposition. In *International Conference on Artificial Intelligence and Statistics*, pp. 726–735. PMLR, 2018.
- jun Liu, Y., Parisot, S., Slabaugh, G., Jia, X., Leonardis, A., and Tuytelaars, T. More classifiers, less forgetting: A generic multi-classifier paradigm for incremental learning. In *ECCV*, 2020.
- Kingma, D. P. and Ba, J. ADAM: A method for stochastic optimization. In *International Conference on Learning Representations*, 2014.
- Kirkpatrick, J., Pascanu, R., Rabinowitz, N., Veness, J., Desjardins, G., Rusu, A. A., Milan, K., Quan, J., Ramalho, T., Grabska-Barwinska, A., et al. Overcoming catastrophic forgetting in neural networks. *Proceedings of the national academy of sciences*, 114(13):3521–3526, 2017.
- Lee, S.-W., Kim, J.-H., Jun, J., Ha, J.-W., and Zhang, B.-T. Overcoming catastrophic forgetting by incremental moment matching. *Advances in Neural Information Processing Systems*, 30:4652–4662, 2017.
- Linderman, S. W., Johnson, M. J., and Adams, R. P. Dependent multinomial models made easy: stick breaking with the pólya-gamma augmentation. In *Proceedings of the 28th International Conference on Neural Information Processing Systems-Volume 2*, pp. 3456–3464, 2015.
- Liu, H., Ong, Y.-S., Shen, X., and Cai, J. When Gaussian process meets big data: A review of scalable gps. *IEEE transactions on neural networks and learning systems*, 31(11):4405–4423, 2020a.
- Liu, Y., Su, Y., Liu, A.-A., Schiele, B., and Sun, Q. Mnemonics training: Multi-class incremental learning without forgetting. In *Proceedings of the IEEE/CVF Conference*

- on *Computer Vision and Pattern Recognition*, pp. 12245–12254, 2020b.
- Mallya, A. and Lazechnik, S. Packnet: Adding multiple tasks to a single network by iterative pruning. In *Proceedings of the IEEE Conference on Computer Vision and Pattern Recognition*, pp. 7765–7773, 2018.
- Mallya, A., Davis, D., and Lazechnik, S. Piggyback: Adapting a single network to multiple tasks by learning to mask weights. In *Proceedings of the European Conference on Computer Vision*, pp. 67–82, 2018.
- McCloskey, M. and Cohen, N. J. Catastrophic interference in connectionist networks: The sequential learning problem. In *Psychology of learning and motivation*, volume 24, pp. 109–165. Elsevier, 1989.
- Minka, T. P. *A family of algorithms for approximate Bayesian inference*. PhD thesis, Massachusetts Institute of Technology, 2001.
- Nassar, J., Linderman, S., Bugallo, M., and Park, I. Tree-structured recurrent switching linear dynamical systems for multi-scale modeling. In *International Conference on Learning Representations*, 2019.
- Polson, N. G., Scott, J. G., and Windle, J. Bayesian inference for logistic models using pólya–gamma latent variables. *Journal of the American Statistical Association*, pp. 1339–1349, 2013.
- Rasmussen, C. E. and Williams, C. K. I. *Gaussian Processes for Machine Learning (Adaptive Computation and Machine Learning)*. The MIT Press, 2005.
- Rebuffi, S.-A., Kolesnikov, A., Sperl, G., and Lampert, C. H. iCaRL: Incremental classifier and representation learning. In *Proceedings of the IEEE conference on Computer Vision and Pattern Recognition*, pp. 2001–2010, 2017.
- Ren, M., Liao, R., Fetaya, E., and Zemel, R. S. Incremental few-shot learning with attention attractor networks. In *Advances in Neural Information Processing Systems*, pp. 5276–5286, 2019.
- Rifkin, R. and Klautau, A. In defense of one-vs-all classification. *The Journal of Machine Learning Research*, 5: 101–141, 2004.
- Rusu, A. A., Rabinowitz, N. C., Desjardins, G., Soyer, H., Kirkpatrick, J., Kavukcuoglu, K., Pascanu, R., and Hadsell, R. Progressive neural networks. *arXiv preprint arXiv:1606.04671*, 2016.
- Schwarz, J., Czarnecki, W., Luketina, J., Grabska-Barwinska, A., Teh, Y. W., Pascanu, R., and Hadsell, R. Progress & compress: A scalable framework for continual learning. In *International Conference on Machine Learning*, pp. 4528–4537. PMLR, 2018.
- Serra, J., Suris, D., Miron, M., and Karatzoglou, A. Overcoming catastrophic forgetting with hard attention to the task. In *International Conference on Machine Learning*, pp. 4548–4557. PMLR, 2018.
- Snell, J. and Zemel, R. Bayesian few-shot classification with one-vs-each pólya-gamma augmented Gaussian processes. *arXiv preprint arXiv:2007.10417*, 2020.
- Snelson, E. and Ghahramani, Z. Sparse Gaussian processes using pseudo-inputs. In *Advances in Neural Information Processing Systems*, pp. 1257–1264. MIT Press, 2006.
- Taitelbaum, H., Chechik, G., and Goldberger, J. Network adaptation strategies for learning new classes without forgetting the original ones. In *IEEE International Conference on Acoustics, Speech and Signal Processing*, pp. 3637–3641. IEEE, 2019.
- Tao, X., Hong, X., Chang, X., Dong, S., Wei, X., and Gong, Y. Few-shot class-incremental learning. In *Proceedings of the IEEE Conference on Computer Vision and Pattern Recognition*, 2020.
- Welinder, P., Branson, S., Mita, T., Wah, C., Schroff, F., Belongie, S., and Perona, P. Caltech-UCSD Birds 200. Technical Report CNS-TR-2010-001, California Institute of Technology, 2010.
- Wenzel, F., Galy-Fajou, T., Donner, C., Kloft, M., and Opper, M. Efficient Gaussian process classification using pólya-gamma data augmentation. In *The AAAI Conference on Artificial Intelligence*, pp. 5417–5424. AAAI Press, 2019.
- Williams, C. K. and Barber, D. Bayesian classification with Gaussian processes. *IEEE Transactions on Pattern Analysis and Machine Intelligence*, 20(12):1342–1351, 1998.
- Wilson, A. G., Hu, Z., Salakhutdinov, R., and Xing, E. P. Deep kernel learning. In *International Conference on Artificial Intelligence and Statistics (AISTATS)*, 2016a.
- Wilson, A. G., Hu, Z., Salakhutdinov, R., and Xing, E. P. Stochastic variational deep kernel learning. In *Proceedings of the 30th International Conference on Neural Information Processing Systems*, pp. 2594–2602, 2016b.
- Wu, C., Herranz, L., Liu, X., van de Weijer, J., Raducanu, B., et al. Memory replay GANs: Learning to generate new categories without forgetting. *Advances in Neural Information Processing Systems*, 31:5962–5972, 2018.
- Xian, Y., Lorenz, T., Schiele, B., and Akata, Z. Feature generating networks for zero-shot learning. In *Proceedings of the IEEE conference on computer vision and pattern recognition*, pp. 5542–5551, 2018.

- Yoon, J., Yang, E., Lee, J., and Hwang, S. J. Lifelong learning with dynamically expandable networks. In *International Conference on Learning Representations*, 2018.
- Yu, L., Twardowski, B., Liu, X., Herranz, L., Wang, K., Cheng, Y., Jui, S., and Weijer, J. v. d. Semantic drift compensation for class-incremental learning. In *Proceedings of the IEEE/CVF Conference on Computer Vision and Pattern Recognition*, pp. 6982–6991, 2020.
- Zhai, M., Chen, L., Tung, F., He, J., Nawhal, M., and Mori, G. Lifelong GAN: Continual learning for conditional image generation. In *Proceedings of the IEEE/CVF International Conference on Computer Vision*, pp. 2759–2768, 2019.

---

# Supplementary Material for GP-Tree: A Gaussian Process Classifier for Few-Shot Incremental Learning

---

## A. Variational Bound & Updates

In section 3.2 we presented the following variational lower bound for the marginal likelihood at each node:

$$\mathcal{C}(\mathbf{c}, \boldsymbol{\mu}, \boldsymbol{\Sigma}) = \mathbb{E}_{p(\bar{\mathbf{f}}|\bar{\mathbf{f}})q(\bar{\mathbf{f}})q(\boldsymbol{\omega})} [\log p(\mathbf{y}|\boldsymbol{\omega}, \bar{\mathbf{f}})] - KL(q(\bar{\mathbf{f}}, \boldsymbol{\omega}) || p(\bar{\mathbf{f}}, \boldsymbol{\omega}))$$

We present the closed-form expression of it and the update rules for the variational parameters  $\boldsymbol{\mu}$ ,  $\tilde{\boldsymbol{\Sigma}}$  and  $\mathbf{c}$ . In the following constants are omitted.

### A.1. Explicit form for the Variational Bound

We will begin with the expectation term:

$$\begin{aligned} & \mathbb{E}_{p(\bar{\mathbf{f}}|\bar{\mathbf{f}})q(\bar{\mathbf{f}})q(\boldsymbol{\omega})} [\log p(\mathbf{y}|\boldsymbol{\omega}, \bar{\mathbf{f}})] \\ & \propto \mathbb{E}_{p(\bar{\mathbf{f}}|\bar{\mathbf{f}})q(\bar{\mathbf{f}})q(\boldsymbol{\omega})} [(\mathbf{y} - \mathbf{1}/2)^T \bar{\mathbf{f}} - \frac{1}{2} \bar{\mathbf{f}}^T \boldsymbol{\Omega} \bar{\mathbf{f}}] \\ & = \mathbb{E}_{q(\bar{\mathbf{f}})q(\boldsymbol{\omega})} [(\mathbf{y} - \mathbf{1}/2)^T \mathbf{K}_{nm} \mathbf{K}_{mm}^{-1} \bar{\mathbf{f}} - \frac{1}{2} Tr(\boldsymbol{\Omega} \mathbf{Q}_{nn}) \\ & \quad - \frac{1}{2} \bar{\mathbf{f}}^T \mathbf{K}_{mm}^{-1} \mathbf{K}_{mn} \boldsymbol{\Omega} \mathbf{K}_{nm} \mathbf{K}_{mm}^{-1} \bar{\mathbf{f}}] \\ & = \frac{1}{2} \{2(\mathbf{y} - \mathbf{1}/2)^T \mathbf{K}_{nm} \mathbf{K}_{mm}^{-1} - Tr(\boldsymbol{\Lambda} \mathbf{Q}_{nn}) \\ & \quad - Tr(\mathbf{K}_{mm}^{-1} \mathbf{K}_{mn} \boldsymbol{\Lambda} \mathbf{K}_{nm} \mathbf{K}_{mm}^{-1} \tilde{\boldsymbol{\Sigma}}) \\ & \quad - \boldsymbol{\mu}^T \mathbf{K}_{mm}^{-1} \mathbf{K}_{mn} \boldsymbol{\Lambda} \mathbf{K}_{nm} \mathbf{K}_{mm}^{-1} \boldsymbol{\mu}\} \end{aligned}$$

Where,  $\lambda_i = \mathbb{E}_{q(\omega_i)}[\omega_i] = \frac{1}{2c_i} \tanh(\frac{c_i}{2})$ ,  $\boldsymbol{\Lambda} = \text{diag}(\lambda_i)$ .

Now, we move to the KL divergence term. Due to independence between  $p(\boldsymbol{\omega})$  and  $p(\bar{\mathbf{f}})$ , and the mean-field as a variational family assumption we have:

$$\begin{aligned} & KL(q(\bar{\mathbf{f}}, \boldsymbol{\omega}) || p(\bar{\mathbf{f}}, \boldsymbol{\omega})) \\ & = KL(q(\bar{\mathbf{f}})q(\boldsymbol{\omega}) || p(\bar{\mathbf{f}})p(\boldsymbol{\omega})) \\ & = KL(q(\bar{\mathbf{f}}) || p(\bar{\mathbf{f}})) + KL(q(\boldsymbol{\omega}) || p(\boldsymbol{\omega})) \end{aligned}$$

The first KL term is between two Gaussian distributions and has the following closed-form expression:

$$\begin{aligned} & KL(q(\bar{\mathbf{f}}) || p(\bar{\mathbf{f}})) \\ & = KL(\mathcal{N}(\boldsymbol{\mu}, \tilde{\boldsymbol{\Sigma}}) || \mathcal{N}(\mathbf{0}, \mathbf{K}_{mm})) \propto \\ & \frac{1}{2} \{Tr(\mathbf{K}_{mm}^{-1} \tilde{\boldsymbol{\Sigma}}) + \boldsymbol{\mu}^T \mathbf{K}_{mm}^{-1} \boldsymbol{\mu} - \log |\tilde{\boldsymbol{\Sigma}}| + \log |\mathbf{K}_{mm}|\} \end{aligned}$$

The second KL term is between two Pólya-Gamma (PG) distributions, each of a mutually independent random variable,

and has a closed-form expression as well:

$$\begin{aligned} KL(q(\boldsymbol{\omega}) || p(\boldsymbol{\omega})) & = \sum_{i=1}^n KL(q(\omega_i) || p(\omega_i)) \\ & = \sum_{i=1}^n KL(PG(1, c_i) || PG(1, 0)) \\ & = \sum_{i=1}^n \log \cosh \frac{c_i}{2} - \frac{c_i}{4} \tanh(\frac{c_i}{2}) \end{aligned}$$

The variational lower bound is obtained by summing all these terms according to Eq. 13.

### A.2. Variational Parameters Update

The update rules for the variational parameters are given by taking the derivative of Eq. 13 w.r.t each of  $\mathbf{c}$ ,  $\boldsymbol{\mu}$ ,  $\tilde{\boldsymbol{\Sigma}}$ . At each iteration, based on a mini-batch of samples  $\mathcal{B}$ , we first update the parameters  $\mathbf{c}^{\mathcal{B}} \subseteq \mathbf{c}$  corresponding to the samples seen in the batch using coordinate ascent scheme while holding  $\boldsymbol{\mu}$ ,  $\tilde{\boldsymbol{\Sigma}}$  fixed. Then,  $\boldsymbol{\mu}$ ,  $\tilde{\boldsymbol{\Sigma}}$  are updated according to a stochastic natural gradient ascent scheme.

The parameters  $\mathbf{c}$  have a unique maximum which is given in a closed-form:

$$c_i = (Q_{ii} + \mathbf{K}_{im} \mathbf{K}_{mm}^{-1} \tilde{\boldsymbol{\Sigma}} \mathbf{K}_{mm}^{-1} \mathbf{K}_{mi} + \boldsymbol{\mu}^T \mathbf{K}_{mm}^{-1} \mathbf{K}_{mi} \mathbf{K}_{im} \mathbf{K}_{mm}^{-1} \boldsymbol{\mu})^{\frac{1}{2}} \quad (16)$$

Where, the subscript  $i$  denotes a specific row/column corresponding to the  $i^{\text{th}}$  sample.

For the parameters  $\boldsymbol{\mu}$ ,  $\tilde{\boldsymbol{\Sigma}}$ , the natural parameterization of the variational Gaussian distribution can be used:  $\boldsymbol{\eta} = \tilde{\boldsymbol{\Sigma}}^{-1} \boldsymbol{\mu}$  and  $\mathbf{H} = -\frac{1}{2} \tilde{\boldsymbol{\Sigma}}^{-1}$ . The update at each batch then becomes:

$$\begin{aligned} \tilde{\nabla}_{\boldsymbol{\eta}} \mathcal{C} & = \frac{n}{2|\mathcal{B}|} \mathbf{K}_{mm}^{-1} \mathbf{K}_{mn}^{\mathcal{B}} (\mathbf{y}^{\mathcal{B}} - \mathbf{1}/2) - \boldsymbol{\eta} \\ \tilde{\nabla}_{\mathbf{H}} \mathcal{C} & = -\frac{1}{2} (\mathbf{K}_{mm}^{-1} + \frac{n}{2|\mathcal{B}|} \mathbf{K}_{mm}^{-1} \mathbf{K}_{mn}^{\mathcal{B}} \boldsymbol{\Lambda}^{\mathcal{B}} \mathbf{K}_{nm}^{\mathcal{B}} \mathbf{K}_{mm}^{-1}) - \mathbf{H} \end{aligned} \quad (17)$$

Where, we used the superscript  $\mathcal{B}$  to denote only the rows/columns of samples in the batch. Note that the natural gradient updates maintain the positive-definiteness of  $\tilde{\boldsymbol{\Sigma}}$ .

## B. Learning Algorithm

Here, we summarize the learning algorithm of GP-Tree with VI and deep kernel learning.

**Algorithm 1** GP-Tree Inference with VI

---

**Input:** Data  $\mathcal{D} = (\mathbf{X}, \mathbf{y})$ ,  $I_1$  number of training iterations with a NN,  $I_2$  Number of training iterations with GP-Tree  
**Init:**  $\mathcal{G}_\theta$  a NN parameterized by  $\theta$   
**For**  $i = 1, \dots, I_1$ :  
  - Sample a mini-batch of data from  $\mathcal{D}$   
  - Learn  $\mathcal{G}_\theta$  with a classification loss  
**End for**  
**Build** GP-Tree  $\mathcal{T}$  as described in section 3.1  
**Init:** GP hyper-parameters  $\phi$ , variational parameters  $\mathbf{c}, \boldsymbol{\eta}, \mathbf{H}$ , and inducing locations  $\bar{\mathbf{X}}$  in the embedded space  
**For**  $i = 1, \dots, I_2$ :  
  - Sample a mini-batch of data from  $\mathcal{D}$   
  - Obtain embedding for  $\mathbf{X}$  with  $\mathcal{G}_\theta(\mathbf{X})$   
  - Traverse the tree (e.g., via in-order traversal)  
  **For** each node in the path:  
    - Update  $\mathbf{c}$  according to Eq. 16  
    - Update  $\boldsymbol{\eta}, \mathbf{H}$  according to Eq. 17  
  **End for**  
  - Update  $\theta, \phi$  and  $\bar{\mathbf{X}}$  using Eq. 15 and by replacing the marginal likelihood terms with the variational lower bound  $\mathcal{C}(\mathbf{c}, \boldsymbol{\mu}, \boldsymbol{\Sigma})$  per node  
**End for**  
**Return**  $\mathcal{G}_\theta, \mathcal{T}, \bar{\mathbf{X}}$

---

## C. Experimental Setup

This section provides further details about the experiments shown in section 5.

### C.1. Inference with Gibbs sampling - Sec. 5.1

**Data.** We used the pre-trained features extracted by (Xian et al., 2018) for the CUB 200-2011 dataset (Welinder et al., 2010). The CUB 200-2011 dataset contains 200 classes of bird species in 11,788 images with approximately 30 examples per class in the training set. Here, since the training set size is limited, we used all 5994 training instances according to the official split and, we split the predefined test set to 2897 samples for validation and 2897 for testing.

**Hyperparameter tuning.** For all baselines, in all experiments, we applied a grid search over the kernel type, either normalized linear kernel or normalized RBF kernel (Snell & Zemel, 2020). We consistently found that under this setting the linear kernel generated better results (this was not true in other settings). The output scale for the linear kernel was chosen based on a grid search in  $\{1, 4, 9, 18\}$ . We used 20 Gibbs chains for the experiments with  $\{4, 6, 8, 10, 20\}$  classes, 10 Gibbs chains for the experiments with 30 classes, and 1 Gibbs chain for the experiments with  $\{40, 50, 60\}$  classes. For the OVE baseline, we were able to use only 10 chains for the experiments with 8 classes and 3 chains for the experiments with 10 classes. These experiments were

done on an NVIDIA V100 32GB GPU. We applied 1 Gibbs sampling step before taking  $\omega$  for the predictive distribution calculations. In these experiments we often found it useful to make predictions with a single sample at the expected value location instead of using the 1D Gaussian-Hermite quadrature.

### C.2. Learning GPs with deep kernel learning - Sec. 5.2

In all experiments we trained from scratch a ResNet-18 (He et al., 2016) adjusted for CIFAR images size with a final embedding layer size of 1024. The Batch size was set to 256. We used SGD with a momentum of 0.9 and a scheduler that decays the learning rate by a factor of 0.1 at epochs 100 and 150. We allocated 10% from the training set for validation using stratified sampling and applied early stopping based on the validation performance. We applied a grid search over the initial learning rate in  $\{0.1, 0.01\}$  for all methods. We found that an initial learning rate of 0.01 was preferred for our method. In GPDNN experiments we also searched for an initial learning rate in  $\{0.001, 0.0005\}$  and experimented with the Adam optimizer (Kingma & Ba, 2014) as well. In all methods, we applied pre-training with a NN only that has a softmax layer after the last embedding layer and the cross-entropy loss. We searched over the number of pre-training epochs in  $\{0, 20, 40, 60, 80\}$ . Either 60 or 80 epochs yielded the best results for our method. For GP-Tree and the GPDNN baseline, we used 40 inducing points per class. For the SV-DKL baseline, we experimented with a grid size of  $\{64, 256\}$ . In all experiments of all methods, we used the RBF kernel over L2 normalized input vectors. In CIFAR-100 experiments of the GPDNN baseline, we also applied an extensive grid search for the probability of labeling error without any success to achieve reasonable accuracy.

### C.3. Class-incremental few-shot learning - Sec. 5.3

**Experimental protocol.** The experiments in this part largely followed the protocol by (Tao et al., 2020) for comparability. We adopted the 10-way 5-shot setting for CUB, the first 100 classes were set as base classes, the remaining 100 classes were split into 10 incremental sessions. For mini-ImageNet, we follow the 5-way 5-shot, with 60 base classes, and 40 novel classes for a total of nine sessions. We used the official train/test split published by (Tao et al., 2020). We pre-allocated a small portion from the training set of the base classes for a validation set. From the CUB dataset, we took 2 samples per class. From the mini-ImageNet dataset, we allocated 5% using stratified sampling. In CUB experiments we fine-tuned a pre-trained ResNet-18 on ImageNet while in mini-ImageNet experiments we trained it from scratch. The final embedding layer size was set to 512. The mini-batch size at the first session was set to 128 in experiments on both datasets. In later sessions, the mini-batch size included

Table 4. Class-incremental few-shot learning on CUB-200-2011. Tree construction variants. Test accuracy averaged over 10 runs.

Method	Sessions										
	1	2	3	4	5	6	7	8	9	10	11
Session Tree	69.74	63.96	59.88	55.28	51.78	48.73	46.60	44.68	42.40	40.94	39.37
Rebuild Base Tree	69.74	62.85	58.81	54.56	51.37	48.50	46.69	45.01	42.56	40.92	39.84
GP-Tree	69.74	<b>64.43</b>	<b>60.55</b>	<b>56.01</b>	<b>52.73</b>	<b>49.95</b>	<b>47.68</b>	<b>46.09</b>	<b>43.82</b>	<b>42.5</b>	<b>41.09</b>

all available samples. We used SGD with a momentum of 0.9.

**Hyperparameter tuning.** For the experiments on GP-Tree, SDC (Yu et al., 2020) and PODNet (Douillard et al., 2020), we applied a grid search over the initial learning rate of the first session in {0.1, 0.01, 0.001}. In CUB experiments it was set to 0.01. In mini-ImageNet experiments, it was set to 0.1. At the first session, we trained the models for 100 epochs with a scheduler that decreased the learning rate by a factor of 0.1 at epochs 40 and 60. At later sessions, for our method, there is nothing to set as it doesn’t require any learning. In SDC and PODNet experiments we trained for 100 epochs and followed the training protocols suggested by each. For SDC, we applied a grid search over  $\gamma$ , the hyperparameter that controls the trade-off between the metric learning loss and the other losses in {1e4, 1e6}. For this baselines, we found it beneficial to start with a few epochs of training using a softmax layer and the cross-entropy loss and only afterwards train with the triplet loss as advocated in the paper. When training with the triplet loss, we also needed to optimize the ratio of positive and negative examples at each batch to make it work.

**GP-Tree configurations.** In GP-Tree experiments, on the initial session, we first applied a few epochs of training using a NN only with a softmax layer and the cross-entropy loss. Then, after 20 epochs in CUB experiments, and 40 epochs in mini-ImageNet experiments, we transitioned to learning with GP-Tree as described in section 3. We used 5 inducing points per class and the RBF kernel on all GPs with an initial length-scale of 1 and an initial output-scale of 4. Here, as well, the inputs to the kernel were normalized by their L2 norm. During training, we assigned a weight to the loss term at each node that is inversely proportional to the amount of data used by that node for inference. On few-shot sessions, we applied the Gibbs sampling variant of our model. We used 30 Gibbs chains and 10 sampling steps. Here we also used the RBF kernel with a fixed length-scale of 1 and a fixed output-scale of 8. At the end of each few-shot session, we saved the 512 dimensional representation of the samples for later sessions.

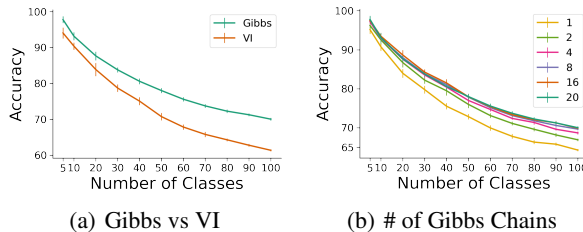


Figure 4. Test accuracy on increasing number of classes. **Left** Gibbs sampling vs variational inference, **Right** varying the number of Gibbs chains. Results are the average over 10 runs ( $\pm$  SEM) on pre-trained features of samples from the CUB 200-2011 dataset.

## D. Additional Experiments

### D.1. GP-Tree Inference

The performance of GP-Tree depends on several factors. Here, we test (1) the effect of using VI against using a Gibbs sampler and, (2) the effect of the number of Gibbs chains. Both analyses were made by observing the test accuracy on the CUB-200-2011 dataset under the setup presented in section 5.1. The results are shown in Figure 4. Figure 4(a) shows a large performance gap in favor of the Gibbs sampling. This result is not surprising since the Gibbs sampler, asymptotically, samples from the correct posterior while in VI we use an approximate one. The figure also shows that the gap is amplified as the number of classes increases. This result is another justification for using Gibbs sampling when learning novel classes under the incremental learning setup. Figure 4(b) shows that as we increase the number of chains the accuracy increase as well; however, the difference is marginal when using four chains or more.

### D.2. Sensitivity Analysis on FSCIL

In the experiments of GP-Tree under the setup of class-incremental few-shot learning, we made several design choices. Here, we examine some of them. We will show that GP-Tree is fairly robust to these choices.

**Tree construction.** You may recall that on the FSCIL setup after learning on the base classes we retain the original tree intact, and at each novel session  $t$ , we build a sub-tree from

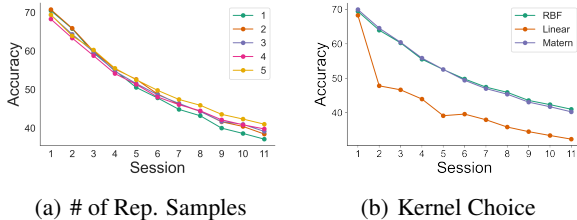


Figure 5. Test accuracy in class-incremental few-shot learning as a function of the number of representative samples per class (left) and the kernel choice (right). Results are the average over 10 runs on the CUB 200-2011 dataset.

samples representations that appeared in sessions  $D_2, \dots, D_t$ . We then connect this sub-tree to the base classes tree with a shared root node. In Table 4 we present two alternatives for the tree construction used for inference during novel sessions ( $t > 1$ ). (1) *Session Tree*; Instead of building a tree from samples in all sessions  $D_2, \dots, D_t$ , in each session build a tree only from classes that appeared at that session. Then, we connect this sub-tree with the tree that is already built via a shared root. (2) *Rebuild Base Tree*; At the end of base training,  $t = 1$ , use the inducing inputs to rebuild the base tree and fit a GP at each node with the Gibbs sampling variant of our approach. Then, at each novel iteration, follow the protocol described briefly at the beginning of this paragraph and section 3.4. Table 4 shows that both alternatives yield good results; however, the approach chosen for GP-Tree is superior.

**Kernel analysis.** The results presented in the main paper for few-shot class-incremental learning were with the RBF kernel and 5 representative samples per class. Here we investigate both choices in Figure 5. Figure 5(a) compares between 1 – 5 representative samples per class. The figure shows that all alternatives achieve high accuracy on all sessions; however, as expected, when using less representative samples there is a slight degradation in performance. This is more prominent in later sessions. Figure 5(b) shows a comparison between the RBF, Matern and Linear kernels. Similar to (Snell & Zemel, 2020) we found gain in normalizing the inputs to the kernels by their L2 norm. Therefore, we applied this method in all settings and for all kernel choices. However, unlike in the few-shot learning case presented in (Snell & Zemel, 2020), in which the normalized linear kernel (also referred to as cosine kernel in that study) yielded the best results, in our case either the RBF kernel or the Matern kernel are preferred by a large margin, especially on novel sessions. We hypothesize that on the base classes the NN outputs a representation that is more linearly separable. Therefore, all kernels perform similarly on them. However, the representation of novel classes is more mixed in the embedding space. Therefore, a stronger kernel that generates non-linear decision boundaries is required.

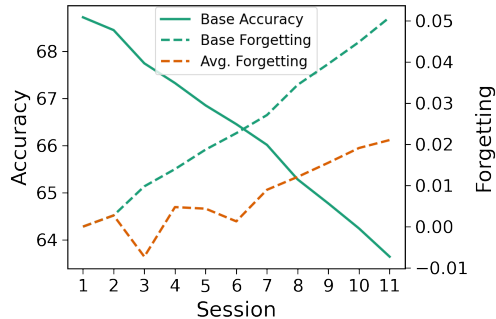


Figure 6. Base accuracy (solid line), base forgetting and, average forgetting across sessions. Results are the average over 5 runs on the CUB 200-2011 dataset.

### D.3. Forgetting Across Sessions

In this part, we examine how GP-Tree performance changes across sessions. To do so, we look at the *average forgetting* (Chaudhry et al., 2018) and the accuracy on base classes as training progress. The average forgetting was designed to estimate the forgetting of prior tasks. Let  $\alpha_j^k$  denote the accuracy of the learner on the  $j^{th}$  task at session  $k > j$ , the forgetting of the  $j^{th}$  task is defined as  $g_j^k = \max_{l \in \{1, \dots, k-1\}} \alpha_j^l - \alpha_j^k$ . This quantity is measured for every task  $j$  seen thus far at each new session. Then, to get an estimate of the average forgetting we may use:  $\frac{1}{k-1} \sum_{j=1}^{k-1} g_j^k$ . Figure 6 shows the accuracy on base classes, the forgetting of base classes and, the average forgetting of all classes across all 11 sessions on the CUB 200-2011 dataset. From the figure, we notice that the accuracy on base classes between the initial and the last session drops by  $\sim 5\%$  and the forgetting, on base classes and in general, is minor.